Journal of the European Ceramic Society 18 (1998) 2313–2321

PII: S0955-2219(98)00237-4
0955-2219/99/$—see front matter

High Oxidation Resistance of Hot Pressed Silicon Nitride Containing Yttria and Lanthania

Frédéric Monteverde* and Alida Bellosi

CNR-IRTEC, Research Institute for Ceramics Technology Via Granarolo 64-48018 Faenza (Ra), Italy

Abstract

Oxidation tests were carried out on Si_3N_4–La_2O_3–Y_2O_3 hot pressed ceramics up to 1500°C. Morphological and analytical characterizations were performed on surfaces and reaction scales after oxidation and correlated with the oxidation kinetics. (Near)-parabolic behaviour was observed at temperatures <1450°C for short periods, while for higher temperatures and longer exposures the kinetics shifted to a linear behaviour. Moreover the excellent oxidation resistance (as demonstrated by extremely low weight gains), particularly up to 1450°C, was related to the high refractoriness of the grain boundary phases in this additive system. Strength degradation after oxidation at several temperatures was also studied and discussed. © *1999 Elsevier Science Limited. All rights reserved*

1 Introduction

The increasing interest for silicon nitride-based ceramics in high temperature structural applications prompted closer investigations of the materials' oxidation resistance. In fact non-oxide ceramics and notably pure silicon nitride (SN) are well known to be inherently unstable and to oxidize at high temperature growing a protective silica-based scale: the use of silica-forming ceramics, thermally stable and hardly permeable to the oxygen and other contaminants recalled, therefore great attention.[1] Composition and amount of the sintering aids play a crucial role on designing materials with tailored and even more powerful performances, markedly if dedicated to operate in severe applications. In fact the oxidation resistance of the multiphase SN ceramics has been often stressed to be strongly influenced by type and content of their intergranular phases.[1–8] Diffusion mechanisms through the growing silica-based scale or the bulk ceramic, being slower than the gas transport or chemical surface reactions, were generally related to the observed (near)-parabolic behaviours.[1,2,5–8] The most favoured explanation considers the inward diffusion of the oxygen (forming silica) and the outward diffusion of intergranular cations (due to the chemical potential gradient) as the rate-controlling mechanisms of the oxidation. However non parabolic kinetics were often observed and many open arguments, despite plentiful published data, still await to be completely clarified.[4,9–12]

Independently of the rate-controlling mechanism, the real components have to fulfil several requirements (e.g. long-term oxidation resistance, creep resistance, low gas permeability, oxidation induced flaw tolerance) and be able to bear severe corrosive conditions which adversely affect the materials' integrity. A substantial open problem is to predict the effects of the oxidation on the flaws' population during service in order to be able to determine the lifetime of a particular component. New modelling strategies on corrosion science have been developing in order to take this into account and to refine models which up to now failed to predict long-term behaviour.[1,9–14]

The purpose of this study is to compare and discuss the oxidation behaviour of materials in the system Si_3N_4–Y_2O_3–La_2O_3 differing in the content of the additives and to correlate the strength degradation (after oxidation) to the involved phenomena.

2 Experimental Procedures

SN-based materials were hot-pressed in vacuum at 1850°C and 30 MPa from commercial powders: Si_3N_4 (UBE-SNE10, Japan), La_2O_3 (Merck, Germany), Y_2O_3 (HC Starck—grade C, Germany). The starting composition of the two materials produced was:

*To whom correspondence should be addressed.

$Si_3N_4 + 2$ wt% $Y_2O_3 + 2$ wt% La_2O_3 (labelled LY22)

$Si_3N_4 + 3$ wt% $Y_2O_3 + 3$ wt% La_2O_3 (labelled LY33).

Both the final hot pressed bodies were fully dense and contained only traces of crystalline intergranular phases. After annealing tests (1400°C for 6 h in flowing nitrogen), traces of crystalline La–Y–Si–O–N phases were also found. A striking feature of these materials is the high temperature strength (up to ~800 MPa measured in air at 1400°C); details on processing, microstructure and mechanical tests are reported elsewhere.[15]

The oxidation cycles were conducted in static air under isothermal conditions for 30 h using a Netzsch thermobalance (weight accuracy ±0·01 mg) up to 1500°C. The heating rate was 20°C min^{-1}. The specimens were cooled down by turning off the furnace. All test pieces were selected with suitable dimensions for exposure in the thermobalance, polished up to 1 μm, carefully washed and weighed with an analytical balance (accuracy ±0·02 mg) before and after oxidation. A thin Platinum ring was fitted between the specimen and the holder (alumina) of the thermobalance in order to avoid the contact of the two ceramic bodies.

The microstructure of the as-oxidized surfaces and of the polished cross sections was examined by SEM-EDS and XRD (Cu-Kα radiation).

In order to examine the mechanical decay of these materials after oxidation, the room temperature strength of bars (2·0×2·5×25 mm) after thermal treatments for 50 h in laboratory air at 1200, 1300 and 1400°C was measured.

3 Results and Discussion

3.1 Oxidation kinetics

Under the testing conditions both the materials showed a high oxidation resistance with very small mass gains even upon oxidation at 1500°C (Table 1). The measured mass gains are comparable with data reported for additive-free HIPped SN[7,8,10] and at least one order of magnitude smaller than hot-pressed SN with other additives.[4,5,10,16–19]

After 30 h, the weight gain versus the oxidation temperature plot (Fig. 1) shows, up to 1450°C, similar trends for both the tested materials, the values being lower than 0·3 mg cm^{-2}; increasing the temperature up to 1500°C, the weight change did not exceed 0·4 mg cm^{-2} for sample LY22, while it reached ~1 mg cm^{-2} for sample LY33.

At temperatures < 1200°C no detectable mass changes indicated that the presence of La–Y–Si oxynitrides within the intergranular phases had negligible influence on the oxidation resistance.

Oxidation of non-oxide ceramics are conventionally monitored by mass change experiments either dynamically or intermittently performing weighing–heating–cooling cycles. However, dealing with extremely low mass changes, it is worth to underline that instrumental drifts (e.g. baseline shifts, buoyancy effects, Pt evaporation) may interfere with the on-line acquisition of the weight change even though the measuring apparatus is able to appreciate such weight variations.

In order to ensure more reproducibility of the experimental data, specific isothermal cycles were scheduled. It was possible to build thermogravimetric curves which, up to 1450°C, are nearly parabolic while, raising the temperature up to 1500°C, the kinetics showed a first parabolic stage (5–10 h) followed by a linear stage. Examples of two different behaviours are shown in Fig. 2.

On the basis of the experimental data and assuming parabolic kinetics up to 1450°C, the calculated rate constants K_p (Table 1) assessed the high oxidation resistance of these materials, in comparison to

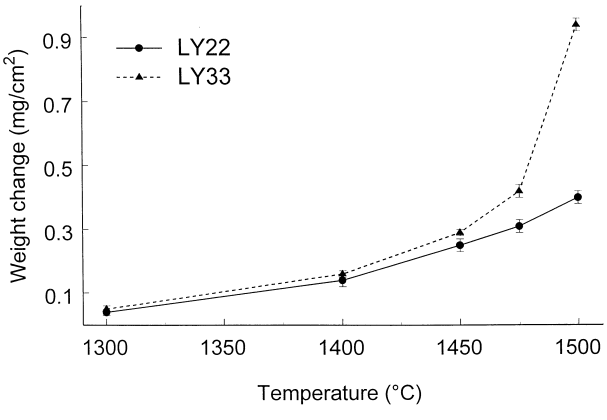

Fig. 1. Weight gain versus oxidation temperature plot of the two tested materials (exposure time: 30 h).

Table 1. Mass gains ΔM (mg cm^{-2}), the relative parabolic rate constant K_p (mg^2 cm^{-4} s^{-1}), the apparent activation energy E_A in the range 1300–1450°C (KJ mol^{-1}) and thickness range τ(μm) of the reation scale after oxidation in static air for 30 h

	LY22					*LY33*				
	1300°C	*1400°C*	*1450°C*	*1475°C*	*1500°C*	*1300°C*	*1400°C*	*1450°C*	*1475°C*	*1500°C*
$\Delta m(10^{-1})$	0·4 ± 0·1	1·4 ± 0·2	2·5 ± 0·2	3·1 ± 0·2	4·0 ± 0·2	0·5 ± 0·1	1·6 ± 0·1	2·9 ± 0·1	4·2 ± 0·2	9·4 ± 0·2
$K_p(10^{-7})$	0·15	1·8	5·8	—	—	0·23	2·4	7·8	—	—
τ	0·4–0·6	1–2	2–4	0·5–1·0	1–1·5	2–3	5–6	8–10	4–7	
	$E_A = (545 \pm 2)$ KJ mol^{-1}					$E_A = (526 \pm 10)$ KJ mol^{-1} (except 1500°C)				

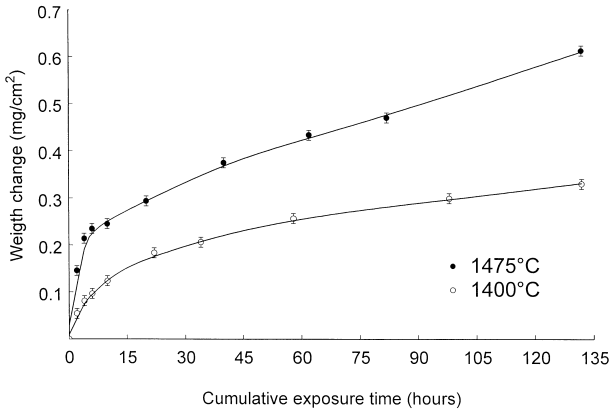

Fig. 2. Thermogravimetric curves of sample LY33 at 1400 and 1475°C.

the data found in literature.[4,5,7,10,16–18]

From these values, through the Arrhenius equation which relates the parabolic rate constants K_p of the reaction with the temperature T, the apparent activation energies in the temperature range 1300–1450°C (Table 1) were estimated.

3.2 Characterization of the oxidation scale

3.2.1 Surface characterization

X-ray diffraction on the oxidized surfaces [Fig. 3(a)] showed, besides $\beta - Si_3N_4$ arising from the unreacted bulk, α-cristobalite in increasing amounts with the increase of the temperature and a crystalline phase (labelled *LaY*), not yet listed in the JCDD diffraction files.

Quantitative analyses from EDS–SEM spectra offered a first answer to the stoichiometry of the *LaY* phase: $Y_2La(SiO_4)_{2.25}$ or $(Y_{2/3}La_{1/3})_2Si_2O_7$. Intrinsic difficulties on obtaining flat mirrored cross sections of the reaction scale and the strong Si K_α signal arising from the silica 'background' yielded such a uncertainty on the mentioned stochiometries. The structure of this 'new' phase has analogies with a known monoclinic phase [$La_2Si_2O_7$, file JCDD no 44–346, space group $P2_1/c$ (14)]. In order to solve the structure of the *LaY* phase and its stoichiometry a direct synthesis from a powder mixture of amorphous silica and the oxides used as additives (La_2O_3 and Y_2O_3) was carried out in a laboratory kiln at 1600°C for 1 h in air: the formation of the *LaY* phase was confirmed [Figs 3(b) and 4] and further crystallographic analyses are in progress.

At low temperatures (< 1200°C), no (crystalline) oxidation products were detected. The absence of surface cracking or buckling confirmed the thermal stability of the Y–La–Si oxynitride intergranular phases. Partial decomposition of them occurred and is evidenced by the formation of a surface porosity accompanied by a slight diffusion of additives in correspondence of the grain boundaries [Fig. 5(a)], without the formation of a surface reaction scale.

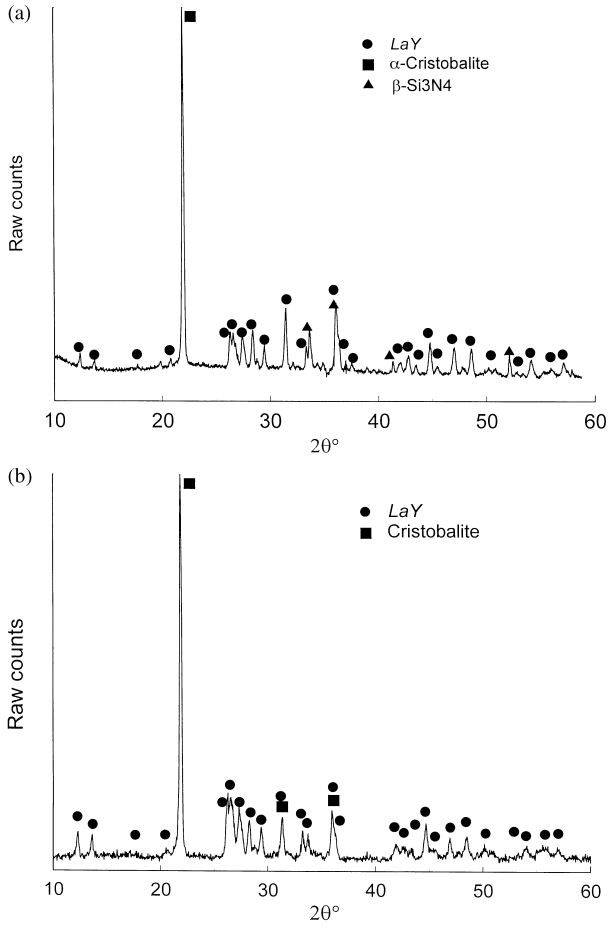

Fig. 3. Unprocessed XRD spectra (a) from the surface of sample LY33 oxidized at 1500°C for 30 h in static air and (b) from a mixture of the new synthesized *LaY* phase and α-cristobalite.

At moderate temperatures (1200–1300°C), the surfaces were hardly modified with the localized growth of silica layer, isolated oxidation pits [Fig. 5(b)] and small oxide mounds exuded from grain boundaries [Fig. 5(c)]. Under the adopted experimental conditions, these reactions at grain boundaries did cause neither cracking (or even spalling) at the surface nor weight change.

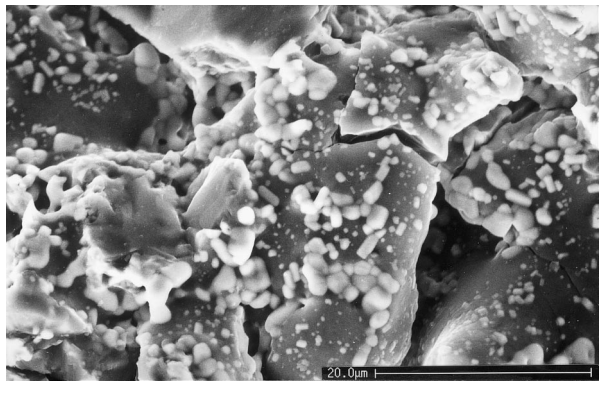

Fig. 4. SE micrograph showing bright islands (*LaY* phase) anchored on grey blocks (α-cristobalite).

From 1300°C up to 1450°C, the surfaces appeared smooth and continuous with polycrystals (*LaY* phase) of various morphologies [Fig. 6(a) and (c)] embedded in a glassy matrix (Y–La silicate); burst nitrogen bubbles were rarely found.

Faceted polycrystals like *LaY* can form in high viscosity glasses, as also previously observed in oxide scales of SN containing yttria and silica or yttria and alumina:[5,16,18] after the nucleation, the growth of these polycrystals proceeds, when the ionic mobility is low, along energetically favoured directions. In fact, yttrium and lanthanum ions are modifiers[20] of the glassy silicates and raise their viscosity. The globular shaped *LaY* polycrystals predominate in consequence of their partial dissolution in the glassy silicate during exposure while faceted shapes appeared mostly at the surface close to the edges of the test piece because of favourable conditions of preferential growth.

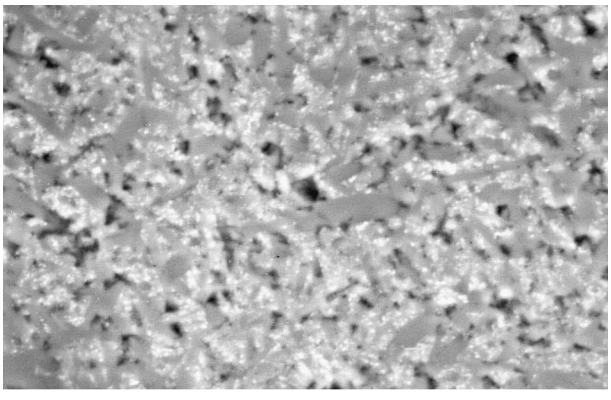

(a)

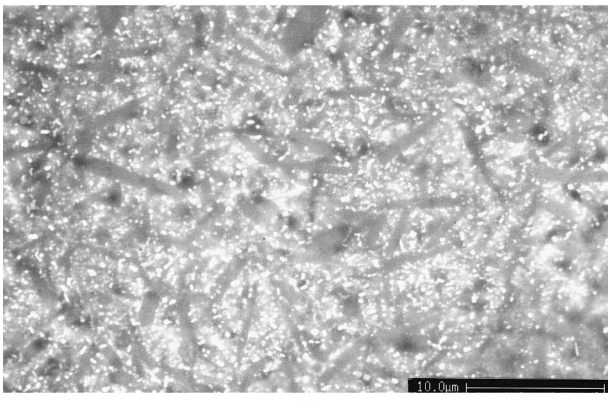

(b)

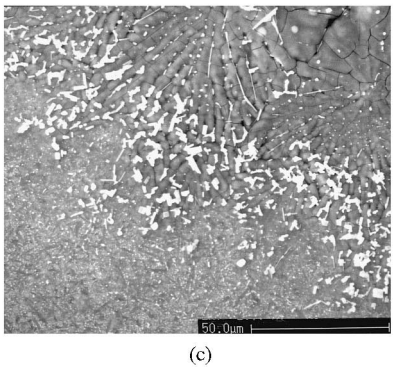

(c)

Fig. 5. BSE micrographs from surfaces of sample LY33 oxidized in air for 30 h at (a) 1000°C and (b,c) 1300°C.

The exact nature of the crystallization is dependent on the local concentration of chemical species (i.e. additives, impurities) and on experimental conditions (temperature, time, atmosphere, glass viscosity, ion or molecular diffusivity): all these features control locally the nucleation and the growth of crystalline compounds in the forming reaction scale.

It has to be noted that the oxide scales of all the samples oxidized at $T > 1300$°C showed thin microcracks probably due to $\beta \rightarrow \alpha$ cristobalite phase transformation on cooling and to residual stresses (not elastically released) arising from volume expansion mismatch between the α-SiO_2 and the *LaY* phase or between the reaction scale and the SN matrix. Increasing temperature up to 1500°C the surfaces became rougher. Burst nitrogen bubbles were frequently observed while the microcrack network enlarged its width due to thicker oxide scale [Fig. 6(b) and (d)].

3.2.2 Cross section analyses

Scales formed up to 1450°C showed a continuously graded structure from the top of the scale towards the bulk of the unreacted SN, similarly in the two tested materials [Fig. 7(a) and (b)]. *LaY* polycrystals were present all over the scale embedded in a glassy matrix (Y/La silicate) with the tendency to concentrate close to the outer surface.

Scales formed at 1475 and 1500°C resulted irregular and rough, particularly in sample LY33 [Fig. 8(a) and (b)]. The formation of new defects (pores, cavities, bubbles, cracks) outlined a distinct boundary between the oxidation product layer and the unreacted SN matrix; large pits up to 20 μm accumulating impurities and additives had formed near below the reaction interface.

Especially for $T \geq 1450$°C [an example is shown in the cross section of Fig. 7(b)], the outer oxide scale is connected to an inner subscale containing pockets and channels entering in the bulk, both composed of Y/La-rich silicates. Under this subscale, a layer of the bulk has grown into a porous one, depleted of the initial intergranular phases; this feature became even more evident as the temperature increased. The presence of such a depleted zone was also previously observed in rare-earth doped Sialon ceramics after oxidation at 1350°C.[19] The enrichment of La and Y cations in the subscale towards the reaction interface is due to their diffusion through the intergranular network; it is favoured by high temperatures which allow the increase of the mobility of the additive cations. The driving force for this diffusion is known to be not only the concentration gradient of these cations

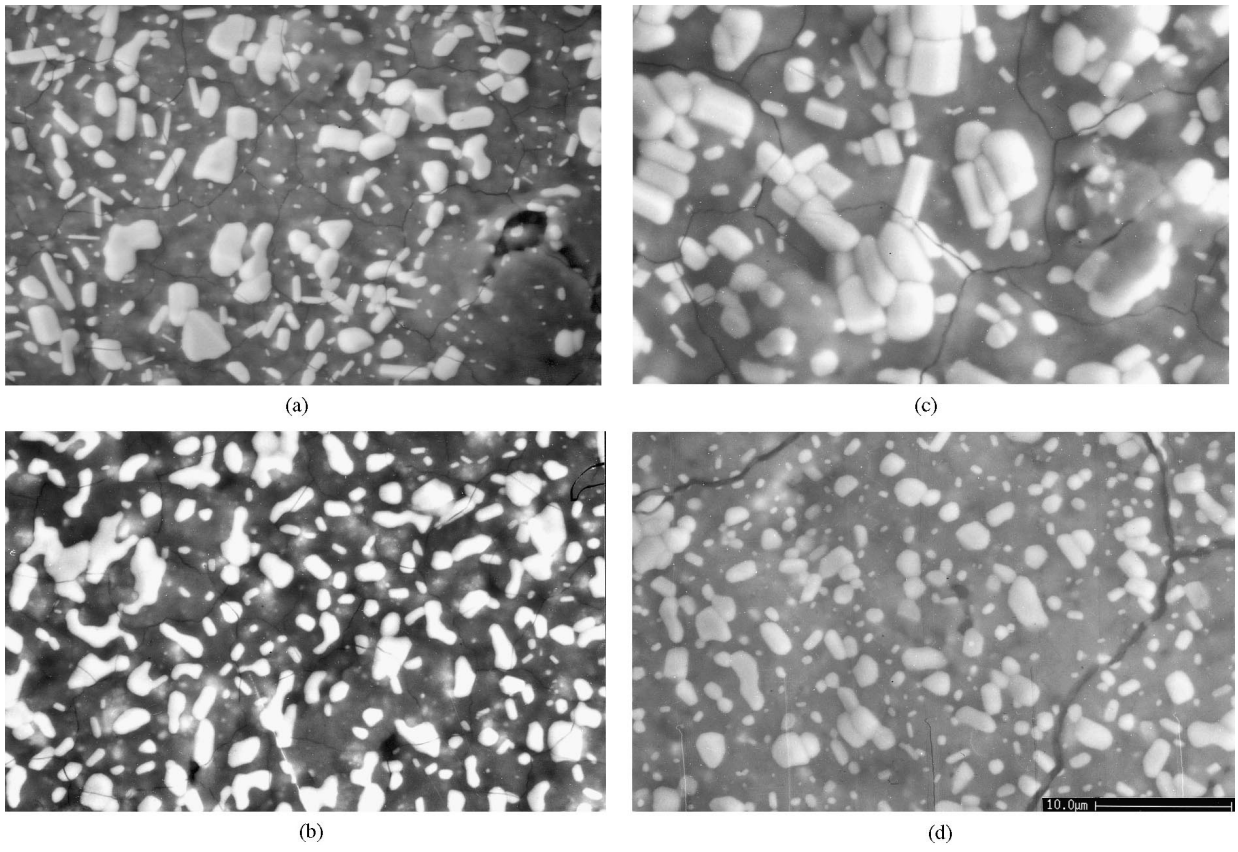

Fig. 6. BSE micrographs from surfaces of samples LY22 (leftside) and LY33 (rightside) oxidized in air for 30 h at (a)–(b) 1450°C and (c)–(d) 1500°C.

(causing a counterdiffusion of oxygen) but also the decrease in free energy of formation of crystalline silicates in the silica-based oxidation layer (i.e. glassy silicate). The viscous silicate, formed on the surface in the early stages of oxidation, clearly penetrates along the intergranular paths (Fig. 7(b)) and favours a fast transport of oxidants towards the bulk. The consequent internal oxidation provides large amount of nitrogen which diffuses through the mentioned channels and the scale towards the atmosphere, as evidenced by the presence of escape pores. The irregular morphology of the oxidation front [Fig. 7(a) and (b)] probably depend on a non uniform composition of the viscous silicate or of the grain boundary phases. The above mentioned features account for the non protective nature of the reaction scale and for the shift from the initial parabolic trend to a linear one with increasing exposure time. From the oversaturated viscous silicate on the surface several crystalline La–Y silicates nucleate and grow with typical morphologies early commented.

As from the X-ray diffraction spectra, at the highest temperature (1500°C) the content of crystalline cristobalite greatly raised up while *LaY* phase decreased. Two hypotheses can be suggested: the amount of diffused La and Y cations (notwithstanding their high mobility) is relatively low, if compared with the massive production of silica (enhanced oxidation of SN, favoured by the deep penetration through the bulk of the less viscous silicate); the partial dissolution of *LaY* polycrystals precipitated in an early stage of oxidation (confirmed by their rounded shape).

Special insight has to be placed on several factors evolving during the studied phenomena. In consequence of the presence of different diffusing species, of the crystallization of cristobalite and other compounds, the characteristics of the reaction scale change dynamically, modifying the available diffusional paths, the solubility and permeability of oxygen and nitrogen, the viscosity of the silicate glass and its interaction with the SN grains.

In order to explain the remarkable oxidation resistance up to 1450°C of these materials in comparison to SN with different additive systems, several and important features have to be pointed out. The limited mobility of the Y and La ions, related to the refractoriness of the intergranular phases in the hot pressed materials reduces the cation diffusivity. Moreover, up to 1450°C, the viscosity of the silicate glass formed on the surface, being higher than other SN-based materials, hinders its penetration and of oxidants along the grain boundaries with an overall effect to slow down the reaction rates, in accordance to the measured values. However, for temperatures higher

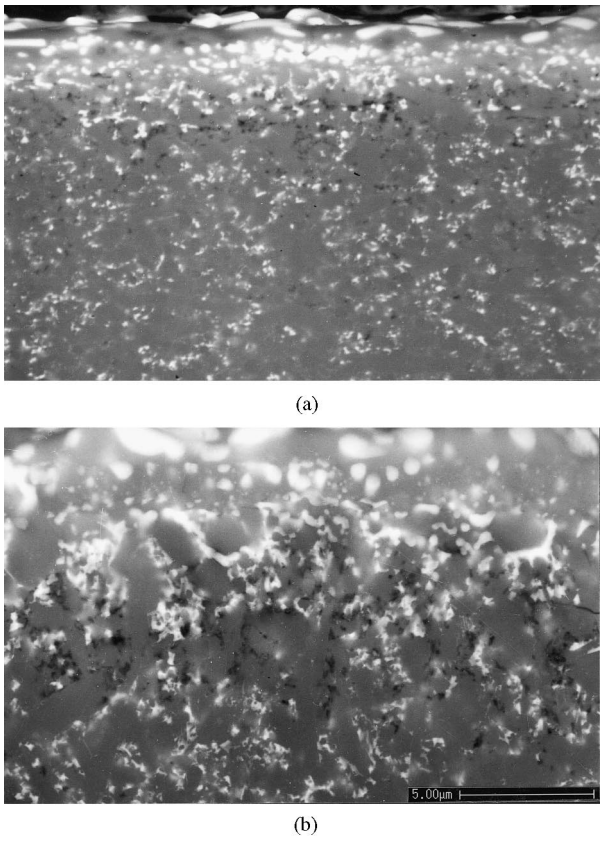

(a) (b)

Fig. 7. BSE micrographs of polished cross section, showing the graded structure of the reaction scale, in samples (a) LY22 and (b) LY33 at 1450°C for 30 h in air.

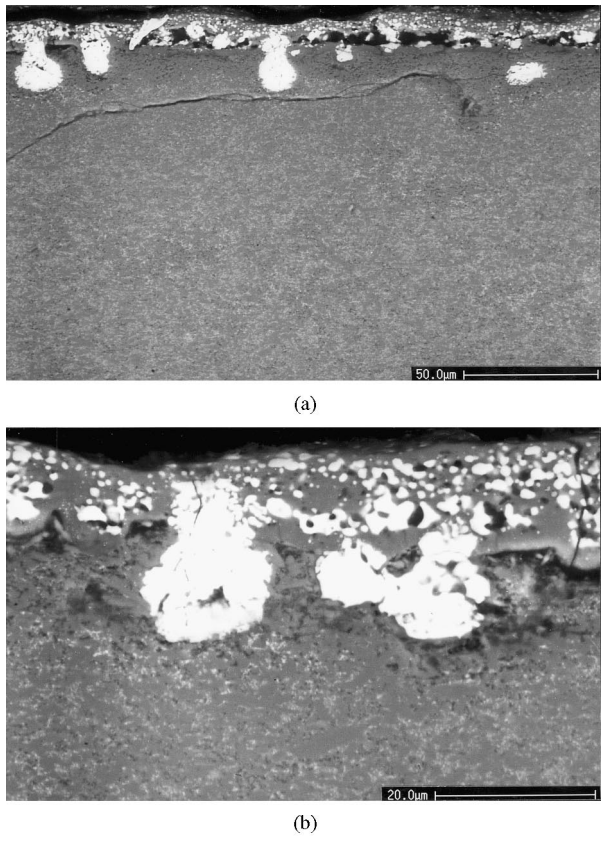

(a) (b)

Fig. 8. BSE micrographs of polished cross section from sample LY33 oxidized at 1500°C in air for 30 h: (a) large view and (b) magnified area.

than 1450°C, the reaction scale starts to be damaged by escape pores and cracks and partially loses its protective function. These new flaws allow the viscous/liquid silicate, available in notable amount, to penetrate more easily and to open the grain boundary channels. The oxidation of the unexposed SN bulk, enhanced by the fast oxygen transport through the viscous silicate and illustrated by the linear trend of the kinetics (Fig. 2), is supposed to become the slowest step of the process. The penetration of a viscous/liquid silicate along the grain boundaries was previously observed during specific tests on the interaction between SN and silicate glasses.[21] It was assessed that a solid/liquid system characterized by high wettability is susceptible to grain boundary penetration during which the ceramic body can dissolve or eventually disintegrate upon exposure to the liquid, the energetics and kinetics of the process being governed by the chemistries at the interface and of the liquid.

The dissolution of the SN grains in the viscous/liquid silicate may occur at high temperatures because the chemical composition of the grain boundary film of the hot pressed samples is not in equilibrium with that of the oxidation products on surface, so a driving force exists as a step toward adjusting the composition of the surface silicate. This reaction can be synergic to the oxidation of the SN bulk and probably assumes considerable influence at temperatures to which the lower viscosity of the glassy silicate formed in the early stages and consequently favours a better wettability of the solid (i.e SN grains).

Keeping in mind all these aspects, besides the composition, also the total volume of the grain boundary phases plays an important role, particularly at $T > 1450$°C where the weight gain of sample LY33 is twice that of LY22: the minimisation of the residual intergranular phase volume impairs the reaction probability and reduces the flux of the out-diffusing ions. Therefore, the reduction of the oxidation damage in polyphase SN ceramics at elevated temperatures in air can be obtained by microstructural engineering, through the selection of sintering aids which improves the refractoriness of the intergranular phase and the reduction of its amount as possible in view to obtain fully dense and fine grained materials. When they are exposed to oxidizing conditions at which the glassy silicate formed on surface lowers its viscosity or is even liquid, extensive oxidation, dissolution and eventually disintegration of SN may simultaneously occur, also when high refractory systems are involved. For the investigated system, this temperature resulted about 1450°C.

Table 2. Flexural strength measured in 4-pt bending fixture, 20 mm as outer span, 10 m as inner span, crosshead speed 0·5 mm min^{-1}

#	σ_T (MPa)				σ_{ox} (MPa)		
	Measured at various temperatures T *on as-produced materials*[15]				*Measured at room temperature after oxidation of the test bars for 50 h*		
T	*RT*	*1000°C*	*1200°C*	*1400°C*	*1200°C*	*1300°C*	*1400°C*
LY22	1137 ± 65	889 ± 119	789 ± 32	678 ± 57	844 ± 63	808 ± 88	557 ± 63
LY33	941 ± 67	826 ± 29	974 ± 71	771 ± 56	747 ± 118	777 ± 74	525 ± 50

Mean value ± standard deviation.

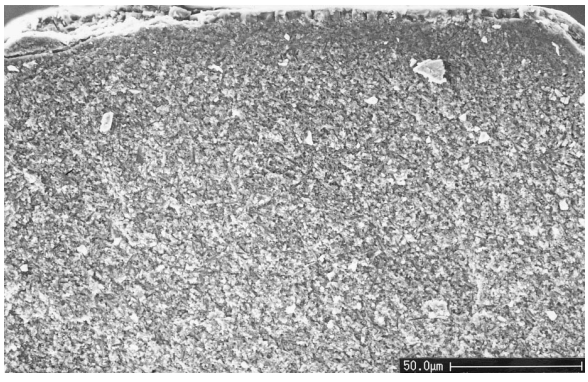

Fig. 9. SE micrograph from a fractured bar (sample LY33) oxidized in air at 1400°C for 50 h: the chamfered edge, from which critical crack started, is visible on the upperside.

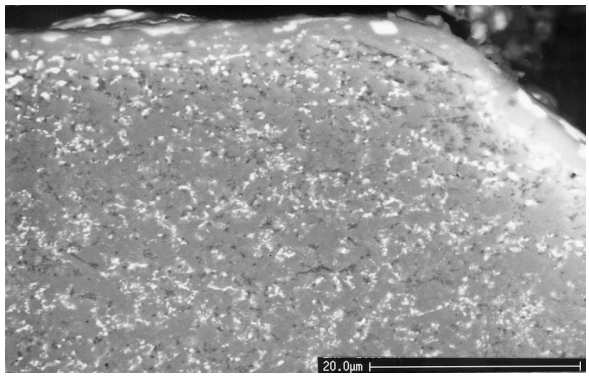

Fig. 10. BSE micrograph from the polished cross section of bar (sample LY33) oxidized at 1400°C for 50 h: clearly new pores have formed close to the chamfered edge (right upper corner).

3.3 Flexural strength degradation after oxidation

The data of flexural strength measured at room temperature on bars oxidized under different conditions are listed in Table 2 and compared to the strength of the as-produced materials. Each strength value represents the average of five test bars.

From the data it appears a decrease in room temperature strength of 26 to 51% (sample LY22) and 21 to 44% (sample LY33) relative to the mean strength of the as-produced materials. The inherent flaw population of the as-machined bars was obviously modified after the oxidative exposure, as new defects (cracks, cavities, additive-depleted and glassy phase-rich zones, oxidation pits) nucleated and grew up. The relief of the machining residual stresses, the oxidation and pitting due a localized corrosion on surface, near-surface and internal, the diffusion and the reaction of chemical species (additives and impurities) from grain boundary, the cavitation, the presence of thermal stresses or cracking induced by thermal expansion anisotropy, the healing of pre-existing cracks and the devitrification of the grain boundary phases are factors which evolve simultaneously during oxidation, really modify the surface status of the bars: it becomes very difficult to evaluate with certainty each individual contribution.

From some fractography analyses, it was observed that most of the fracture origins in samples oxidized at temperatures up to 1300°C were pre-existing flaws. In this case, the main contribution for the strength degradation corresponded to the residual stress relaxation[15] which in these materials was measured to be in the order of 100–200 MPa.[22] Remarking the strength values exceeding 500 MPa after 50 h of exposure at 1400°C in air for SN-based materials, the significant strength degradation was connected to new defects,[23] mainly located in correspondence of the chamfered edges (Fig. 9), or at their corners (Fig. 10), of the tensile loaded surfaces: these sites likely suffered from the machining treatment a local stress concentration which allowed new defects to nucleate or pre-existing ones to grow faster than in less stressed areas.

4 Conclusions

The oxidation behaviour at high temperature (up to 1500°C) of the hot-pressed Si_3N_4–Y_2O_3–La_2O_3 system was studied. An excellent oxidation resistance under thermal treatment (30 h) up to 1450°C was verified by low weight gains ($< 0{\cdot}3$ mg cm^{-2}) and explained in term of low volume and refractoriness of the grain boundary phases and reduced mobility of the additive cations. The oxidation followed, up to 1450°C, a nearly parabolic law: the oxide scale resulted protective and the overall process was governed by diffusional mechanisms. At higher

temperatures, after a short initial parabolic stage, the rate controlling mechanism was supposed to be the oxidation of silicon nitride: the kinetics, characterized by a linear trend, can be ascribed to a reaction-controlled process. This evidence suggested that the reaction scale, increasing exposure time, became non-protective: it could probably be related to the porous nature and to the disruption of the scale (e.g. due to nitrogen bubble's bursting) allowing oxygen to diffuse through cracks and burst bubbles. Transported along the grain boundary channels by the viscous/liquid silicate formed on surface the oxygen easily reaches subscale regions, creating an internal oxidation front. It cannot be excluded a synergic phenomenon due to the penetration of the viscous/liquid silicate which wets and dissolves the SN grains.

A monoclinic crystalline compound (Y–La silicate), not yet listed in the JCDD diffraction files, was found among the oxidation products and was successfully synthesized.

The exposure of these materials to oxidizing atmosphere at temperatures in the range 1200–1300°C for 50 h decreased the fracture strength of about 20%. A new defect population (cracks, cavities, glassy-phase rich regions, additive depleted zones), generated in the (sub)-surface at temperatures higher than 1300°C, controlled the substantial strength degradation.

The comparison of the results confirmed that a reduction (from 6 to 4 wt%) of the additive content may significantly improve the long term stability at very high temperatures of SN hot-pressed with $Y_2O_3 + La_2O_3$ as sintering aids.

Acknowledgements

The authors acknowledge helpful discussions with Dr G. Celotti on XRD data processing, Mr D. Dalle Fabbriche for assistance on furnace running, Dr S. Guicciardi and Mr C. Melandri for technical support on mechanical tests.

References

1. Luthra, K. L., Some new perspectives on oxidation of silicon carbide and silicon nitride. *J. Am. Cer. Soc*, 1991, **74**(5), 1095–1103.
2. Gogotsi, Y. G. and Grathwohl, G., Stress enhanced oxidation of silicon nitride ceramics. *J. Am. Cer. Soc*., 1993, **76**(12), 3093–3104.
3. Riley, F. L., The corrosion of ceramics: where do we go from here? In *Key Engineering Materials*, Vol. 113, ed. R. J. Fordham, D. J. Baxter and T. Graziani. Trans Tech Publications, 1996, pp. 1–14.
4. Gogotsi, Y. G., Grathwohl, G., Thümmler, F., Yaroshenko, V. P., Herrmann, M. and Taut, C., Oxidation of yttria and alumina-containing dense silicon nitride ceramics. *Journal of the European Ceramics Society*, 1993, **11**, 375–386.
5. Bellosi, A., Oxidation behaviour of nitrides and borides as monolithic and composite ceramics. In *Corrosion of Advanced Ceramics: Measurement and Modelling*, NATO ASI Series, Vol. 267, ed. K. G. Nickel. Kluwer Academic, Dordrecht, 1994, pp. 131–142.
6. Jacobson, N. S., Corrosion of silicon-based ceramics in combustion environments. *J. Am. Cer. Soc*., 1993, **66**(1), 3–28.
7. Chen, J., Sjöberg, J., Lindqvist, O., O'Meara, C. and Pejryd, L., The rate-controlling processes in the oxidation of HIPped silicon nitride with and without sintering additives. *Journal of the European Ceramics Society*, 1991, **7**, 319–327.
8. Backhaus Ricoult, M. and Gogotsi, Yu G., Identification of oxidation mechanisms in silicon nitride ceramics by transmission electron microscopy studies of oxide scales. *J. Mat. Res*., 1995, **10**(9), 2306–2321.
9. Nickel, K. G., Multiple law modelling for the oxidation of advanced ceramics and a model-independent figure of merit. In *Corrosion of Advanced Ceramics: Measurement and Modelling*, NATO ASI Series, Vol. 267, ed. K. G. Nickel. Kluwer Academic, Dordrecht, 1994, 59–71.
10. Käll, P.-O., Nygren, M. and Persson, J., Non parabolic oxidation kinetics of advanced ceramics. In *Corrosion of Advanced Ceramics: Measurement and Modelling*, NATO ASI Series, Vol. 267, ed. K. G. Nickel. Kluwer Academic, Dordrecht, 1994, pp. 73–84.
11. Tressler, R. E., Theory and experiments in corrosion of advanced ceramics. In *Corrosion of Advanced Ceramics: Measurement and Modelling*, NATO ASI Series, Vol. 267, ed. K. G. Nickel. Kluwer Academic, Dordrecht, 1994, pp. 3–22.
12. Ogbuji, L. U. J. T., The oxidation process in silicon nitride. In *Corrosion of Advanced Ceramics: Measurement and Modelling*, NATO ASI Series, Vol. 267, ed. K. G. Nickel. Kluwer Academic, Dordrecht, 1994, pp. 117–129.
13. Luthra, K. L., Theoretical aspects of the oxidation of silica-forming ceramics, In *Corrosion of Advanced Ceramics: Measurement and Modelling*, NATO ASI Series, Vol. 267, ed. K. G. Nickel. Kluwer Academic, Dordrecht, 1994, pp. 23–34.
14. Nordberg, L. O., Käll, P.-O. and Nygren, M. A., Mathematical analysis of the non-parabolic oxidation behaviour of the α-sialon matrices and composites. In *Key Engineering Materials*, Vol. 113, ed R. J. Fordham, D. J. Baxter and T. Graziani. Trans Tech Publications, 1996, pp. 39–48.
15. Bellosi, A., Monteverde, F. and Babini, G. N., Influence of powder treatment methods on sintering, microstructure and properties of silicon nitride-based materials. In *Engineering Ceramics '96: Higher Reliability through Processing*, NATO ASI Series, Vol. 25, ed. G. N. Babini *et al*. Kluwer Academic, 1997, 197–212.
16. Bellosi, A., Babini, G. N., Li-Ping, H. and Xi-Ren, F., Phase effects on oxidation resistance in Si_3N_4–Al_2O_3–Y_2O_3. *Mat. Chem. Phys*., 1990, **26**, 21–33.
17. Klemm, H., Tangermann, K., Schubert, C. and Hermel, W., Influence of molybdenum silicide additions on high temperature oxidation resistance of silicon nitride materials. *J. Am. Cer. Soc*., 1996, **79**, 2429–2435.
18. Bellosi, A. and Galassi, C., Factors influencing the thermal stability of Si_3N_4–Al_2O_3–Y_2O_3 ceramics in oxygen environments. *Materials Engineering*, 1990, **1**(3), 949–958.
19. Shen, Z., Käll, P.-O. and Nygren, M., Oxidation behaviour of yttrium and rare-earth doped α-sialon ceramics at 1350°C. In *Key Engineering Materials*, Vol. 132–136. Trans Tech Publications, 1997, pp. 1576–1579.
20. Kingery, W. D., Bowen, H. K. and Uhlmann, D. R., *Introduction to Ceramics*, 2nd ed. J. Wiley & Sons, New York, 1976.

21. Esposito, L., Saiz, E., Tomsia, A. P. and Cannon, R. M., High temperature colloidal processing for glass metals and glass/ceramic FGM's. In *Proc. Ceramic Microstructure '96: Control at the Atomic Level*, ed. A. P. Tomsia and A. M. Glaeser. Plenum Press, New York, 1997.
22. Johnson-Walls, D., Evans, A. G., Marshall, D. B. and James, M. R., Residual stresses in machined ceramic surfaces. *J. Am. Cer. Soc.*, 1986, **69**(1), 44–47.
23. Ukyo, Y., The effect of a small amount of impurity on the oxidation of Si_3N_4 ceramics. *J. Mat. Sci.*, 1997, **32**, 5483–5489.